Effect of Dendrimer Generation on the Assembly and Mechanical Properties of DNA/Phosphorus Dendrimer Multilayer Microcapsules

ARTICLE *in* MACROMOLECULES · JULY 2006

Impact Factor: 5.8 · DOI: 10.1021/ma060698m

7 AUTHORS, INCLUDING:

Byoung-Suhk Kim
Chonbuk National University
86 PUBLICATIONS **1,213** CITATIONS
SEE PROFILE

Kaloian Koynov
Max Planck Institute for Polymer Research
121 PUBLICATIONS **1,920** CITATIONS
SEE PROFILE

Anne-Marie Caminade
French National Centre for Scientific Research
554 PUBLICATIONS **9,914** CITATIONS
SEE PROFILE

Olga I Vinogradova
Russian Academy of Sciences
111 PUBLICATIONS **3,350** CITATIONS
SEE PROFILE

Effect of Dendrimer Generation on the Assembly and Mechanical Properties of DNA/Phosphorus Dendrimer Multilayer Microcapsules

Byoung-Suhk Kim,[†] Olga V. Lebedeva,[†] Kaloian Koynov,[†] Haofei Gong,[†] Anne-Marie Caminade,[‡] Jean-Pierre Majoral,[‡] and Olga I. Vinogradova*,[†,§]

Max Planck Institute for Polymer Research, Ackermannweg 10, Mainz 55128, Germany, Laboratoire de Chimie de Coordination CNRS, 205 route de Narbonne, 31077 Toulouse Cedex 04, France, and A. N. Frumkin Institute of Physical Chemistry and Electrochemistry, Russian Academy of Sciences, Leninsky Prospect 31, 119991 Moscow, Russia

Received March 28, 2006

ABSTRACT: We report the preparation, characterization and mechanical properties of DNA/phosphorus dendrimer multilayer microcapsules. The shells of these microcapsules are composed by alternating DNA and positively charged dendrimer $G_n(NH^+Et_2Cl^-)_m$ ($n = 1, 2, 3, 4$; $m = 12, 24, 48, 96$). The same multilayers were constructed on planar support to examine their layer-by-layer growth and to determine the multilayer thickness. Surface plasmon resonance spectroscopy (SPR) showed regular linear growth of the multilayer film after the first dendrimer layer. We probe the mechanical properties of these DNA/dendrimer microcapsules by measuring force−deformation curves with the atomic force microscope (AFM). The experiment suggests that they are softer than microcapsules assembled from linear flexible polyelectrolytes (PE) studied before. The stiffness of the capsules increases with the generation of used dendrimer. This reflects the change in the multilayer thickness, but not the changes in structure of surface DNA/dendrimer complexes, which almost likely remains similar for all dendrimer generations.

1. Introduction

The complexes of DNA molecules with different types of positively charged entities have attracted attention from scientists in various fields[1] and are important for many applications such as molecular recognition, biological transport, and cell repair.[2−4] DNA molecules form complexes with multivalent cations,[5−7] linear polycations,[8] proteins,[9,10] colloidal particles,[11,12] and lipids.[13,14] Most of the cationic agents forming these complexes and aggregates vary greatly in chemical composition as well as in the number of electric charges, providing for a wide range of different DNA complexes that can be easily assembled and are potentially useful as DNA vectors in novel gene therapies. Viral-based gene delivery is currently one of the most efficient methods to introduce exogeneous genes within cells.[15,16] More recently, cationic dendrimers,[17−23] which also can interact with DNA molecules, have also shown great potential in gene transfection.[22,24] They can also be used as sensors, drug carriers, and more.[25−30]

There has also been some recent interest in using dendrimers as building blocks for the layer-by-layer (LbL) preparation of molecularly thin multilayer films.[31,32] Several attempts have been made to assembly polyelectrolyte (PE)/dendrimer supported multilayers[33,34] and microcapsules.[35,36] However, we are unaware about an investigation of self-assemblies of DNA and dendrimer molecules, except as of some studies of random DNA-dendrimer complexes carried out in bulk solutions.[18,19] Here we try to compensate this lack of experimental data and report an approach to prepare DNA/dendrimer multilayers and multilayer microcapsules. Beside an obvious practical (DNA delivery[37]) interest, the assembly and investigation of physical properties of DNA/dendrimer multilayer films and microcapsules allows one to judge about the interaction of dendrimers with DNA and the nature of complexes formed. In particular, it might give a clue for understanding structural peculiarities of surface DNA/dendrimer composites. In connection to this an important relevant issue is the role of ionic cross-linking in formation and properties of multilayer structures.

In our paper, we are primarily interested in the buildup and mechanical properties of multilayer films composed of layers of alternating DNA and cationic phosphorus-containing dendrimers of several generations. We use a combination of several experimental techniques to show that the mechanical properties of DNA/dendrimer microcapsules differ from the PE/PE, PE/dendrimer, and DNA/PE systems studied before and to explore the influence of the generation of used dendrimer on the structure and the stiffness of multilayer shells.

2. Experimental Section

2.1. Materials. The double-stranded deoxyribonucleic acid sodium salt (DNA; salt-free, lyophilized), purchased from Sigma (Fluka, Germany), is a highly polymerized natural product originating from calf thymus and the form of a white fibrous substance containing less than 5% of protein. A molecular weight for this product is reported to be ca. 6.0×10^6 g/mol, which yields an average size per molecule of ca. 9090 base pairs, equal to a contour length of $\sim 3\ \mu$m. This sample was used without further purification.

The cationic dendrimers used in this study were the *N*,*N*-disubstituted hydrazine phosphorus-containing dendrimers of the first, second, third and fourth generations having 12, 24, 48, and 96 functional groups, respectively, on the surface with cationic character $G_n(NH^+Et_2Cl^-)_m$ ($n = 1-4$, $m = 12-96$; M_w 3200−33700 g/mol). The synthesis, characteristic data and structure formula of $G_n(NH^+Et_2Cl^-)_m$ were reported in refs 17 and 38.

The fluorescent dye fluorescein isothiocyanate (FITC) was purchased from Sigma-Aldrich Chemie GmbH, Germany. Hydrochloric acid (HCl), sodium chloride (NaCl) were purchased from Riedel-de Haën, Germany. All chemicals were of analytical purity or higher quality and were used without further purification. Water

* To whom correspondence should be addressed. E-mail: vinograd@mpip-mainz.mpg.de.
[†] Max Planck Institute for Polymer Research.
[‡] Laboratoire de Chimie de Coordination CNRS.
[§] A. N. Frumkin Institute of Physical Chemistry and Electrochemistry, Russian Academy of Sciences.

10.1021/ma060698m CCC: $33.50
Published on Web 07/08/2006

used for all experiments was purified by a commercial Milli-Q Gradient A10 system containing ion exchange and charcoal stages and had a resistivity of 18.2 MΩ/cm. The pH was measured by using a pH meter (InoLab, Germany) with an accuracy of ±0.5.

Suspensions of monodispersed weakly cross-linked melamine formaldehyde particles (MF-particles) with a radius of $r_0 = 2.0 \pm 0.1$ μm were purchased from Microparticles GmbH (Berlin, Germany). Glass bottom dishes (0.17 mm/o.d. 30 mm) with optical quality surfaces were obtained from World Precision Instruments Inc. (USA). Glass spheres (radius 20 ± 1 μm) were purchased from Duke Sci. Co., California. The coupling prism and the glass substrates used for SPR experiments were made of LaSFN9 glass and were purchased from Hellma Optik, Germany.

2.2. Methods. Capsule Preparation. The DNA/$G_n(NH^+Et_2Cl^-)_m$ capsules were prepared as follows. The positively charged MF particles (50 μL of 10 wt % water dispersion) as a template were incubated with 1 mL of DNA solution (0.5 mg/mL containing 0.5 mol/L NaCl, pH 6) at room temperature for 50 min, followed by three centrifugation/rinsing cycles, and finally dispersed in water. A 1 mL portion of a $G_n(NH^+Et_2Cl^-)_m$ salt-free solution (1 mg/mL, pH 4) was then added to the particle dispersion. After 30 min given for adsorption, three centrifugation/wash cycles were performed (as above). These specific conditions for the dendrimer solution were chosen in order to fully charge the ammonium groups of the dendrimer materials. The DNA and $G_n(NH^+Et_2Cl^-)_m$ adsorption steps were repeated four times each to build multilayers on the MF particles. Each adsorption followed by washing out excess polymer and salt. The microcapsules referred to below as (DNA/$G_n(NH^+Et_2Cl^-)_m)_4$ capsules were obtained by dissolving the MF template in HCl at pH 1.2−1.6 and washing with water three times as described before.

Microscopy. Confocal laser scanning microscopy images were taken with a commercial confocal microscope unit FV300 (Olympus, Japan) used in combination with an inverted fluorescence microscope Olympus IX70. A high-resolution (60×) bright (NA = 1.45) oil immersion objective was used. The drop of suspension of capsules was applied to a glass bottom dish with subsequent adding the water. High resolution and contrast of the confocal images was achieved by the use of the low molecular fluorescent dye FITC added to the capsule solution at a concentration of $\sim 10^{-6}$ mol/L. The excitation wavelength was $\lambda = 488$ nm.

The AFM images of dried capsules deposited on silicon wafers were obtained in a tapping mode (Nanoscope IIIa, Digital Instruments). At least three microcapsules in each sample were imaged. The images were analyzed with Nanoscope 5.30r1 software.

For scanning electron microscopy (SEM) analysis a drop of suspension of capsules was applied to a silicon wafer with sequential drying at room temperature for several hours.[39] The measurements were performed using a Gemini Leo (Zeiss) 1530 instrument operating at a working distance of 2 mm and an acceleration voltage of 0.5 kV. Since the samples were not covered with a gold layer before inspection, this low acceleration voltage was applied in order to avoid charging of the sample. The images were recorded using the InLens detector.

Force Measurements. The experimental setup was described before.[40−42] Briefly, load (force) vs deformation curves were measured with the Molecular Force Probe device (MFP) 1D (Asylum Co., Santa Barbara, CA), which has a nanopositioning sensor that corrects hysteresis and creep of the piezotranslator. For the force measurements we used V-shaped cantilevers (Micromash, Estonia, spring constants $k = 3.0$ N/m). The spring constant of the cantilever was estimated from the resonance frequency calibration plot (Cantilevers catalog, Micromash, Estonia). Glass spheres were glued onto the apex of cantilevers with epoxy glue (UHU Plus, Germany). The capsule deformation experiment has been described before.[42] Here we performed the dynamic measurements at intervals of piezotranslator speed from 0.2 to 20 μm/s. The result of the measurement represents the deflection Δ vs the position of the piezo translator at a single approach. The force F was determined from the cantilever deflection, $F = k\Delta$. As before, we assume that zero separation is at the point of the first measurable force.[43] Then the deformation is calculated as the difference between the position of the piezo translator and the cantilever deflection. The diameter of the capsule was determined optically with an accuracy of 0.2 μm and from the AFM load vs deformation curves (like in ref 43). The relative deformation ϵ of the capsule was then calculated as $\epsilon = 1 - H/(2r_0)$, where H is the minimum sphere/substrate separation.[42,43] To get reliable results, we have performed several series of force measurements. Every series included at least 10 experiments. Then the average of all force vs deformation curves was calculated.

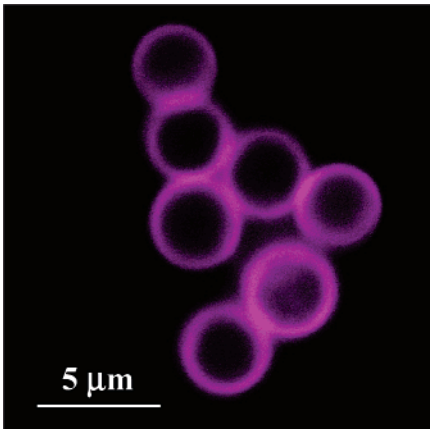

Figure 1. Typical confocal image of the $(DNA/G_3(NH^+Et_2Cl^-)_{48})_4$ microcapsules.

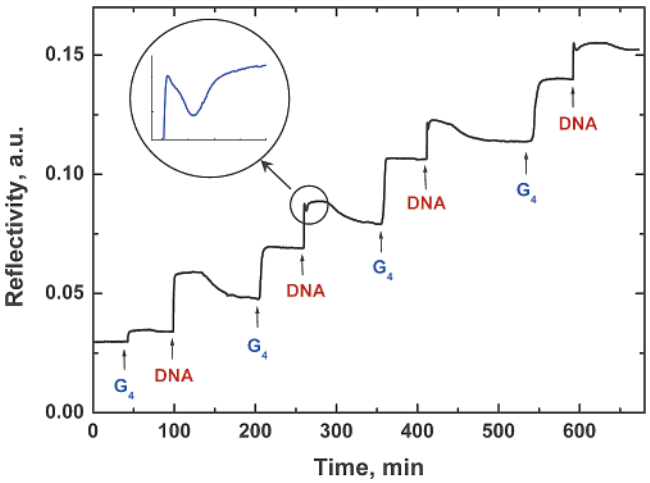

Figure 2. Kinetic SPR scan profile of the consecutive deposition of four bilayers of DNA/$G_4(NH^+Et_2Cl^-)_{96}$. The inset shows a zoom of the selected area of the spectra.

Surface Plasmon Resonance Spectroscopy. To measure the thickness of $G_n(NH^+Et_2Cl^-)_m$/DNA multilayers we used a home-built surface plasmon resonance spectrometer (SPR) and a procedure described before (see ref 44 for more details). The multilayers were assembled on a gold layer functionalized by a monolayer of 3-mercaptopropionic acid (3MPA), according to a procedure described before.[36] The deposition of multilayers was performed in conditions identical to those employed for the capsule preparation. To evaluate a thickness of deposited films we have assumed a constant refractive index of 1.5 for both the DNA and dendrimer layers.

3. Results and Discussion

3.1. General Observations. Typical confocal scanning images of DNA/dendrimer capsules are shown in Figure 2. One can see that they are strongly aggregated, which is similar to what was observed previously for DNA/polyelectrolyte capsules.[45] The absolute majority of capsules (>80%) has an ideal spherical shape. This result represents a successful attempt to

prepare dendrimer-based capsules without protective polyelectrolyte coating. One can expect that the microcapsule shells composed of DNA and dendrimer have the mechanical resistance against the osmotic stress from in the capsule interior, which accompanies the MF dissolutions, and are more stable than previously assembled poly(styrenesulfonate) (PSS)/dendrimer capsules.[36]

3.2. Characterization of the Multilayers. Dendrimer/DNA multilayers analogue to those used for microcapsules preparation were constructed on a planar support in order to characterize their layer-by-layer growth by SPR measurements. Figure 2 illustrates the kinetics of this process for $G_4(NH^+Et_2Cl^-)_{96}$/DNA multilayers. It is seen that the addition of each layer leads to an increase in the reflectivity. The analysis of the plateau regions of the kinetic curves confirms that the adsorption time used during the assembly of microcapsules allows it to reach equilibrium. The washing of the samples leads to a decrease in reflectivity, very small in the case of G4($NH^+Et_2Cl^-$)96 and rather significant for the DNA. The almost instantaneous increase in the reflectivity signal after injection of the DNA or dendrimer solution could originate from either a refractive index change (of the solution vs the pure buffer) or from a rapid adsorption of DNA (dendrimer) to the interface. Since we used concentrations of only 0.5 and 1 mg/mL for the DNA and dendrimer solutions respectively, the first explanation is not very likely. Furthermore, we have performed additional angular SPR scans, which showed that changing the pure buffer with DNA or dendrimer solution does not lead to a shift in the critical angle of total internal reflection[44] This is clear evidence that the increase of reflectivity corresponds to a fast adsorption of a DNA (dendrimer) layer upon the injection of the respective solution. Note that the DNA and the dendrimer show similar adsorption kinetics, but their behaviors during the rinsing with pure water are quite different. Dendrimer layers are quite stable and exhibit minor or no desorption upon washing. In contrast, a significant desorption of DNA molecules or slow conformational rearrangements of the adsorbed DNA layer leading to a decrease in its thickness were found. As can be seen from the inset in Figure 2 after the initial strong growth of the reflectivity associated with DNA adsorption, a small but well pronounced decrease in reflectivity followed by its recovery can be observed within a characteristic time interval of about 3 min. This effect is also observed during the deposition of the second, third, and fourth DNA layers and may be caused by conformational rearrangements of the already deposited film. The kinetics of the LbL deposition of the $G_{1-3}(NH^+Et_2Cl^-)_{12-48}$/DNA films was also studied and showed features similar to those discussed above for the $G_4(NH^+Et_2Cl^-)_{96}$/DNA multilayers.

Figure 3 (top) shows the equilibrium optical thickness of the dendrimer/DNA films as a function of the dendrimer generation. The data reveal regular linear growth of the films after the first dendrimer layer (Figure 3 (bottom)). The significantly smaller thickness of the first dendrimer layer is likely related to a incomplete coverage of the gold surface with the negatively charged, self-assembled monolayer of 3MPA. This may result in a rather incomplete (inhomogeneous) first dendrimer layer with smaller average refractive index. Since a fixed value of refractive index was used for all layers in the SPR analysis, the evaluated optical thickness of this incomplete layer is naturally smaller than those of the other more opaque layers. All DNA layers show the same thickness of about 2.7 nm, which is very close to the cross section of the DNA double helix (~ 2 nm). In our previous work,[45] we have studied PAH/DNA multilayers and have found that on PAH support DNA forms layers with

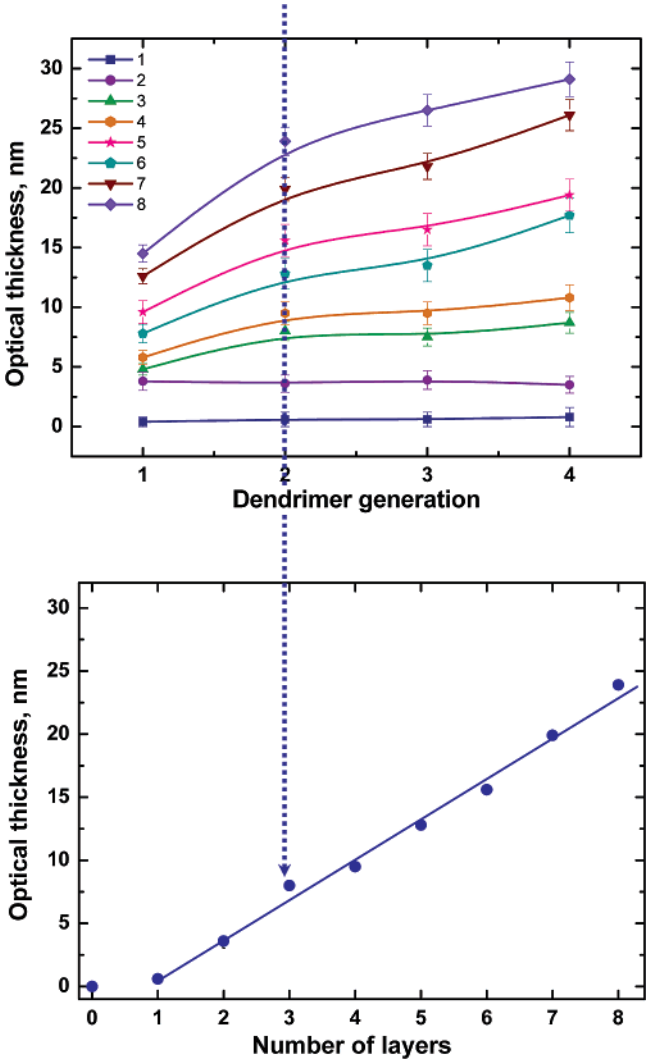

Figure 3. Top: Equilibrium optical thickness of a $G_n(NH^+Et_2Cl^-)_m$/DNA films as a function of dendrimer generation. A numbers of curves correspond to a number of deposited layers. Bottom: Thickness of a $G_2(NH^+Et_2Cl^-)_{24}$/DNA films as a function of deposited layers. Odd layers are from $G_n(NH^+Et_2Cl^-)_m$. Even layers are from DNA.

typical thickness around 6 nm, so that we have concluded that the DNA molecules form a lamellar phase of vertical surface loops. The value obtained here indicates that DNA does not form similar loops on the dendrimer support. For the monolayers of dendrimers G_1, G_2, G_3, and G_4 we evaluated optical thickness as ~2.1, 4.0, 4.3, and 6.5 nm, respectively. Since this is close to the diameter of dendrimers in a bulk solution,[46,47] our result indicates that there is no discernible spreading of dendrimer molecules onto the DNA layer surface.

3.3. Morphology of the Capsules. To investigate the multilayer shell morphology, we have taken and analyzed AFM and SEM images of dried capsules (Figures 4 and 5). AFM images of the surface of DNA/$G_1(NH^+Et_2Cl^-)_{12}$ and DNA/$G_4(NH^+Et_2Cl^-)_{96}$ shells show clearly granule domain structure (Figure 4). The granules likely indicate the structure due to dendrimers and confirm the SPR result that DNA does not form vertical surface loop structure in contrast to the DNA/PAH microcapsules studied before.[45] Note that the morphology of the capsules does not depend on the generation of dendrimers, although of course the size of granules on the surface of DNA/$G_4(NH^+Et_2Cl^-)_{96}$ shells (Figure 4b) is larger in comparison with DNA/$G_1(NH^+Et_2Cl^-)_{12}$ (Figure 4a). Figure 5 shows typical SEM images of dried capsules. The surface of the capsules is

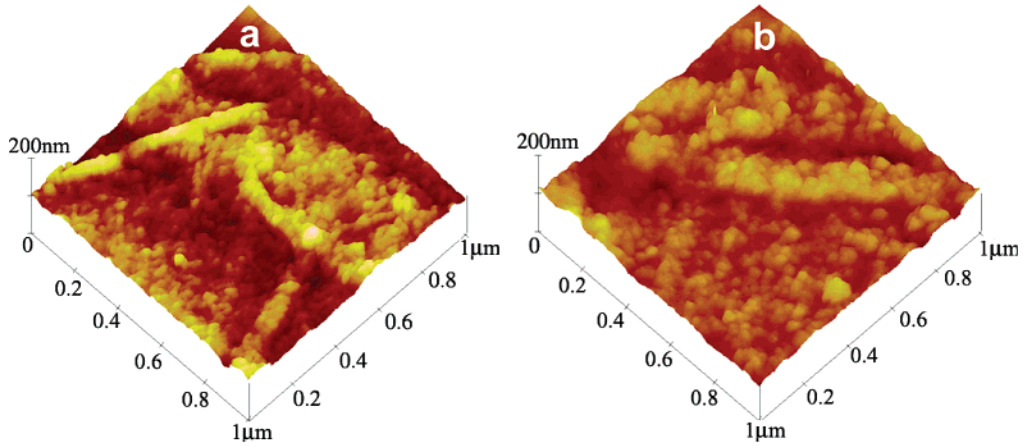

Figure 4. AFM images of dried $(DNA/G_1(NH^+Et_2Cl^-)_{12})_4$ (a) and $(DNA/G_4(NH^+Et_2Cl^-)_{96})_4$ (b) capsules.

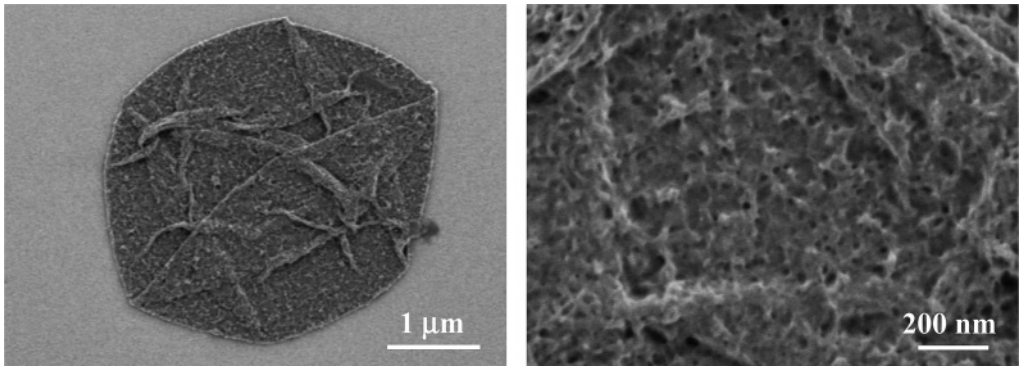

Figure 5. SEM images of dried $(DNA/G_4(NH^+Et_2Cl^-)_{96})_4$ capsules.

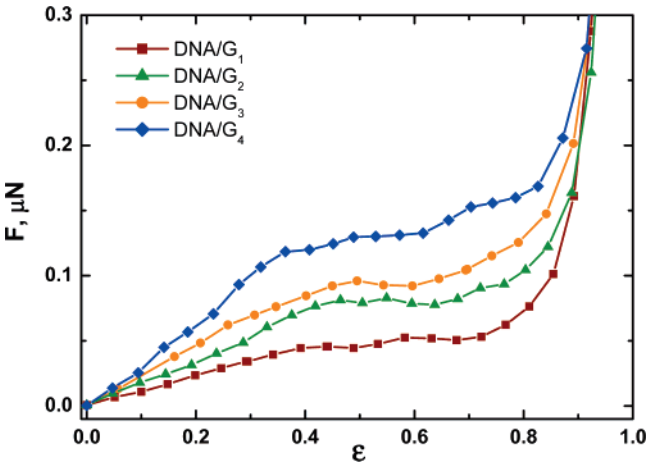

Figure 6. Average force−deformation curve measured for $(DNA/G_n(NH^+Et_2Cl^-)_m)_4$ capsules. Only every 15th point is shown.

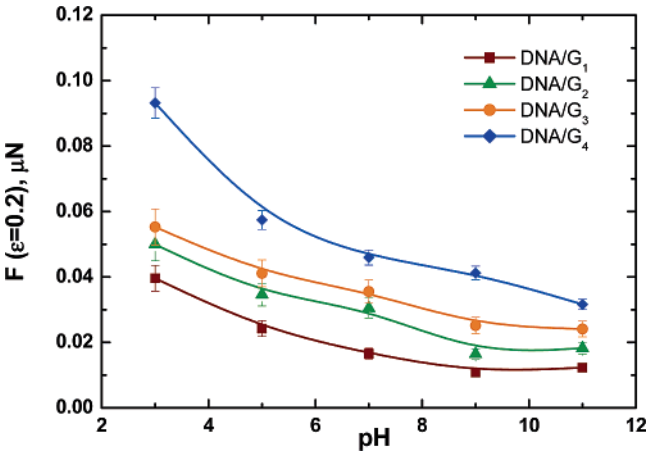

Figure 7. Force at fixed relative deformation ($\epsilon = 0.2$) as a function of pH for $(DNA/G_n(NH^+Et_2Cl^-)_m)_4$. capsules.

quite rough and contains some isolated nanopores. This is different both from smooth PSS/PAH and PSS/dendrimer shells[36,39] and from highly porous DNA/PAH shells studied before.[45]

3.4. Deformation Profiles. Figure 6 shows the average force vs deformation profiles for $(DNA/G_n(NH^+Et_2Cl^-)_m)_4$ microcapsules. One can see that higher generation of dendrimers leads to the increase in the stiffness of the capsules. This result is evidently connected with the increase in shell thickness which increases the force.[48] Another explanation might be a change in the binding modes with the increase of dendrimer generation. According to a simple model[18] for a DNA−dendrimer complexation, the higher dendrimer generation complexes might become more compact since one dendrimer molecule might bind more pieces of DNA helices. In our opinion, our data indicate that such an explanation is unlikely for the multilayers studied. Note that dendrimer/DNA capsules are slightly stiffer than capsules with the same shell thickness made from PSS (or PAH)/dendrimer[36] and DNA/PAH[45] capsules, which probably reflects the fact that they are less permeable due to structure pecularities of DNA/dendrimer complex leading to the practical absence of nanopores and low fragility. They are, however, softer than capsules composed of linear PEs (PSS/PAH) studied before [42,48,49], which is likely because in water environment molecules of $G_n(NH^+Et_2Cl^-)_m$ are not fully charged,[30] so that the amount of ionic cross-links[41] is smaller than for fully charged PSS/PAH multilayers. This is confirmed by the effect of pH posttreatment on the stiffness (Figure 7). At lower pH, where a larger portion of the dendrimer surface groups is protonated,[30] the stiffness

of the capsules increases. Note that for the fourth generation of dendrimer the influence of pH posttreatment is the most pronounced. One can speculate that this is a consequence of a larger amount of charges at the dendrimer interface.

4. Conclusions

We have shown that $(DNA/G_n(NH^+Et_2Cl^-)_m)_4$ microcapsules can be successfully assembled. The microcapsules prepared present novel dual delivery/release systems that are potentially useful for a range of applications. The stiffness of the DNA/$G_n(NH^+Et_2Cl^-)_m$-based shell materials is found to be smaller than that for linear polyelectrolyte/polyelectrolyte (PSS/PAH) microcapsules studied before. The stiffness of the capsules increases with the generation of used dendrimer. This reflects the change in the multilayer thickness, but not the changes in structure of surface DNA/dendrimer complexes, which almost likely remains similar for all dendrimer generations.

Acknowledgment. B.-S.K. and H.G. thank Alexander von Humboldt Foundation for a research fellowship. We are grateful to G. Glasser for taking SEM images.

References and Notes

(1) Alberts, B.; Bray, D.; Lewis, J. R.; M.; Roberts, K.; Watson, J. D. *Molecular biology of the cell*. New York, 1994.
(2) Hayes, J. *Chem. Biol.* **1995**, *2* (3), 127−135.
(3) Behr, J. P. *Acc. Chem. Res.* **1993**, *26*, 274−278.
(4) Miller, A. D. *Angew. Chem., Int. Ed. Engl.* **1998**, *37*, 1768−1785.
(5) Zinchenko, A. A.; Sergeyev, V. G.; Yamabe, K.; Murata, S.; Yoshikava, K. *Chem. Biol. Chem.* **2004**, *5*, 360−368.
(6) Kasyanenko, N. A.; Nikolenko, O. V.; Prokhorova, S. A.; Smorygo, S. A.; Djaschenko, S. A.; Ivin, B. A.; Frisman, E. V. *Mol. Biol.* **1997**, *31*, 240−224.
(7) Kasyanenko, N. A.; Prokhorova, S. A.; Haya Enriquez, E. F.; Sudakova, S. S.; Frisman, E. V.; Dyachenko, S. A.; Smorygo, N. A.; Ivin, B. A. *Colloids Surf. A: Physiochem. Eng. Asp.* **1999**, *148/1S*, 121−128.
(8) Howard, K. A.; Dash, P. R.; Read, M. L.; Ward, K.; Tomkins, L. M.; Nazarova, O.; Ulbrich, K.; Seymour, L. W. *Biochim. Biophys. Acta* **2000**, *1475* (3), 245−255.
(9) Schiessel, H. *J. Phys.: Condens. Matter.* **2003**, *15*, R699−R774.
(10) Nadassy, K.; Wodak, S. J.; Janin, J. *Biochemistry* **1999**, *38*, 1999−2017.
(11) Kneuer, C.; Sameti, M.; Bakowsky, U.; Schiestel, T.; Schirra, H.; Schmidt, H.; M.; L. C. *Bioconjugate Chem.* **2000**, *11*, 926−932.
(12) Jeon, S.; Granick, S. *Colloids Surf. A* **2004**, *238* (1−3), 109−112.
(13) Rädler, J.; Koltover, I.; Salditt, T.; Safinya, C. R. *Science* **1997**, *275* (5301), 810−814.
(14) Koltover, I.; Salditt, T.; Rädler, J.; Safinya, C. R. *Science* **1998**, *281* (5373), 78−81.
(15) Briand, P.; Kahn, A. *Pathol. Biol.* **1993**, *41*, 663−671.
(16) Roessler, B. Y.; Hartman, J. W.; Vallance, D. K.; Latta, Y. M.; Janich, J. L.; Davidson, B. L. *Hum. Genet. Ther.* **1995**, *6*, 307−316.
(17) Loup, C.; Zanta, M. A.; Caminade, A. M.; Majoral, J. P.; Meunier, B. *Chem.−Eur. J.* **1999**, *5*, 3644−3650.
(18) Chen, W.; Turro, N. J.; Tomalia, D. A. *Langmuir* **2000**, *16*, 15−19.
(19) Gössl, I.; Shu, L.; Schlüter, D.; Rabe, J. P. *J. Am. Chem. Soc.* **2002**, *124*, 6860−6865.
(20) Luo, D.; Haverstick, K.; Belcheva, N.; Han, E.; Saltzman, W. M. *Macromolecules* **2002**, *35*, 3456−3462.
(21) Maszewska, M.; Leclaire, J.; Cieslak, M.; Nawrot, B.; Okruszek, A.; Caminade, A. M.; Majoral, J. P. *Oligonucleotides.* **2003**, *13*, 193−205.
(22) Haensler, J.; Szoka, F. C. *Bioconjugate Chem.* **1993**, *4*, 372−379.
(23) Bielinska, A.; Kukowska-Latallo, J. F.; Johnson, J.; Tomalia, D. A.; Baker, J. R. *Nucleic Acids Res.* **1996**, *24*, 2176−2182.
(24) Tomalia, D. A.; Naylor, A. M.; Goddard, W. A. I. *Angew. Chem., Int. Ed. Engl.* **1990**, *29*, 138−175.
(25) Bosman, A. W.; Janssen, H. M.; Meijer, E. W. *Chem. Rev.* **1999**, *99*, 1665−1688.
(26) Majoral, J. P.; Caminade, A. M. *Chem. Rev.* **1999**, *99*, 845−880.
(27) Caminade, A. M.; Majoral, J. P. *Acc. Chem. Res.* **2004**, *37*, 341−348.
(28) Frechet, J. M. J.; Tomalia, D. A. *Dendrimers and other dendritic polymers;* Chichester, U.K., 2001; p 647.
(29) Newkome, G. R.; Vogtle, F.; Moorefield, C. N. *Dendrimers and dendrons*; VCH: Weinheim, Germany, 2001.
(30) Solassol, J.; Crozet, C.; Perrier, V.; Leclaire, J.; Béranger, F.; Caminade, A. M.; Meunier, B.; Dormon, D.; Majoral, J. P.; Lehmann, S. *J. Gen. Virol.* **2004**, *85*, 1791−1799.
(31) Watanabe, S.; Regan, S. L. *J. Am. Chem. Soc.* **1994**, *116*, 8855−8856.
(32) Tsukruk, V. V.; Rinderspracher, R.; Bliznyik, V. N. *Langmuir* **1997**, *13*, 2171−2176.
(33) He, J. A.; Valluzzi, R.; Yang, K.; Dolukhanyan, T.; Sung, C.; Kumar, J.; Tripathy, S. K.; Samuelson, L.; Balogh, L.; Tomalia, D. A. *Chem. Mater.* **1999**, *11*, 3268−3274.
(34) Hernandez-Lopez, J. L.; Bauer, R. E.; Chang, W. S.; Glasser, G.; Grebel-Koehler, D.; Klapper, M.; Kreiter, M.; Leclaire, J.; Majoral, J. P.; Mittler, S.; Müllen, K.; Vasilev, K.; Weil, T.; Wu, J.; Zhu, T.; Knoll, W. *Mater. Sci. Eng., C* **2003**, *23*, 267−274.
(35) Khopade, A.; Caruso, F. *Nano Lett.* **2002**, *2*, 415−418.
(36) Kim, B. S.; Lebedeva, O. V.; Kim, D. H.; Caminade, A. M.; Majoral, J. P.; Knoll, W.; Vinogradova, O. I. *Langmuir* **2005**, *21*, 7200−7206.
(37) Shchukin, D. G.; Patel, A. A.; Sukhorukov, G. B.; Lvov, Y. M. *J. Am. Chem. Soc.* **2004**, *126*, 3374−3375.
(38) Majoral, J. P.; Caminade, A. M.; Maraval, V. *Chem. Commun.* **2002**, *24*, 2929−2942.
(39) Lulevich, V. V.; Nordschild, S.; Vinogradova, O. I. *Macromolecules* **2004**, *37*, 7736−7741.
(40) Lulevich, V. V.; Radtchenko, I. L.; Sukhorukov, G. B.; Vinogradova, O. I. *Macromolecules* **2003**, *36*, 2832−2837.
(41) Lulevich, V. V.; Vinogradova, O. I. *Langmuir* **2004**, *20*, 2874−2878.
(42) Lulevich, V. V.; Andrienko, D.; Vinogradova, O. I. *J. Chem. Phys.* **2004**, *120*, 3822−3826.
(43) Lulevich, V. V.; Radtchenko, I. L.; Sukhorukov, G. B.; Vinogradova, O. I. *J. Phys. Chem.* **2003**, *107*, 2735−2740.
(44) Knoll, W. *Annu. Rev. Phys. Chem.* **1998**, *49*, 569−638.
(45) Vinogradova, O. I.; Lebedeva, O. V.; Vasilev, K.; Gong, H.; Garcia-Turiel, J.; Kim, B. S. *Biomacromolecules* **2005**, *6*, 1495−1502.
(46) Leclaire, J.; Coppel, Y.; Caminade, A. M.; Majoral, J. P. *J. Am. Chem. Soc.* **2004**, *126*, 2304−2305.
(47) Le Berre, V.; Trevisiol, E.; Dagkessamanskaia, A.; Sokol, S.; Caminade, A. M.; Majoral, J. P.; Meunier, B.; François, J. *Nucleic Acid Res.* **2003**, *31*, e88.
(48) Vinogradova, O. I. *J. Phys.: Condens. Matter.* **2004**, *16*, R1105−R1134.
(49) Vinogradova, O. I.; Andrienko, D.; Lulevich, V. V.; Nordschild, S.; Sukhorukov, G. B. *Macromolecules* **2004**, *37*, 1113−1117.

MA060698M